ACS Photonics

Letter

pubs.acs.org/journal/apchd5

True Single-Photon Stimulated Four-Wave Mixing

Shuai Dong,[†] Xin Yao,[†] Wei Zhang,*[,†] Sijing Chen,[‡] Weijun Zhang,[‡] Lixing You,[‡] Zhen Wang,[‡] and Yidong Huang[†]

[†]Tsinghua National Laboratory for Information Science and Technology, Department of Electronic Engineering, Tsinghua University, Beijing, 100084, China

[‡]State Key Laboratory of Functional Materials for Informatics, Shanghai Institute of Microsystem and Information Technology, Chinese Academy of Sciences, Shanghai 200050, China

ABSTRACT: Single-photon stimulated four-wave mixing (StFWM) is an important nonlinear optical phenomenon at the single-photon level. In this process, signal and idler photons are stimulated by seeded single photons when two pump photons are annihilated. The generated photons are correlated with each other, and more importantly, one of them is in the same mode with the seeded photons. Hence, StFWM has great potential to realize complex functions of photonic quantum information processing, such as quantum state manipulation and quantum cloning. In this paper, we provide the first experimental demonstration of single-photon StFWM in a piece of optical fiber. By using heralded single photons as the seeded photons, a true single-photon StFWM process is realized at the telecom band. It is confirmed by time-resolved four-photon coincidence measurement and variation of four-photon coincidence counts under different seed−pump delays. According to the experiment results, the potential performance of a quantum cloning machine based on this process is estimated.

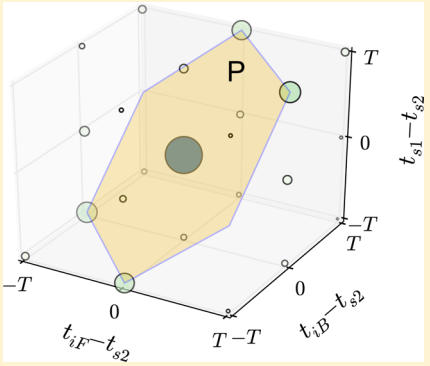

KEYWORDS: *stimulated four-wave mixing, single photons, optical fibers, photon statistics, quantum cloning*

Four-wave mixing (FWM) is an important parametric nonlinear process in media with third-order nonlinearity ($\chi^{(3)}$). In the classical theory of nonlinear optics, the third-order nonlinear polarization terms lead to the nonlinear coupling among the four waves propagating in the medium, which is described by coupled-mode equations.[1] It occurs significantly only when the matching conditions of frequencies and wave vectors are satisfied. It is phase sensitive so that not only the amplitudes but also the phases of the four waves would evolve in this process. Since the observations of FWM over half a century ago,[2] a variety of applications have been proposed and demonstrated, such as parametric amplification,[3] phase conjugation,[4] optical wavelength conversion,[5] and optical signal regeneration.[6,7] It is worth noting that FWM is also an important way to realize squeezed states,[8,9] a type of nonclassical states in quantum optics; hence, it is widely used in the research of quantum metrology and quantum information processing (QIP)[10] based on continuous variables.

If some of the waves in FWM are at the single-photon level, it should be looked at in a quantum way. A widely investigated case is spontaneous FWM (SpFWM), in which two pump photons from the degenerate or nondegenerate strong pump wave(s) are annihilated and two photons with other wavelengths are created from the vacuum fluctuation simultaneously.[11−20] Due to the energy and momentum conservation in this process, the generated photons are correlated. Hence, it is a promising candidate for photonic quantum state generation. Generation schemes for various entangled biphoton states have been demonstrated,[21−29] based on the coherent manipulation or superposition of the correlated state generated via SpFWM. They can be realized in third-order nonlinear media such as optical fibers,[21,22,25,26] integrated waveguides, and resonators based on silicon[27,28] or Si_3N_4,[24] generating biphoton states at the telecom band. SpFWM can also be realized in atomic ensembles, by which generation of photonic quantum states with a subnatural line width is realized.[23] Recently, frequency-uncorrelated biphoton states are generated via SpFWM in a dispersion tailored waveguide,[30] showing its flexibility in applications of quantum light sources.

If not only strong pump wave(s) but also single-photon level waves are injected into the nonlinear medium, other types of FWM could be expected. A well-known example is the FWM Bragg scattering. In this process, the two pump waves are nondegenerate, a pump photon at a specific frequency is annihilated, while a new pump photon at the other pump frequency is created. At the same time, the input single photon is also annihilated with the creation of a new photon with different frequency. Hence, it can be used to realize the frequency conversion of single photons,[31] which is an important and challenging task in photonic QIP. Recently, this has been demonstrated experimentally.[32,33] In this paper, our attention is focused on another process: single photon stimulated FWM (StFWM). In this process, two pump photons are annihilated (whether they are degenerate or non-

Received: December 21, 2016
Published: March 24, 2017

DOI: 10.1021/acsphotonics.6b01020
ACS Photonics 2017, 4, 746−753

degenerate), while a pair of signal and idler photons are stimulated by the seeded single photons. They are not only correlated with each other but also correlated with the seeded photons. It can be expected that single-photon StFWM could largely extend the applications of FWM for photonic QIP, from only the biphoton state generation to more complex applications, such as quantum state manipulation,[34] optimal quantum cloning,[35,36] and multiphoton entanglement generation.[37,38] Especially, this process is preferred to telecom band QIP since it could be realized in third-order nonlinear waveguides and resonators at the telecom band. Recently, Agarwal et al. demonstrated that phase-sensitive amplification could be applied on time-bin entangled photon pairs to improve their transmission over optical fibers.[39] It is essentially an application of StFWM in which the seeded state is a biphoton state. However, to the authors' knowledge, the observation of StFWM stimulated by single seeded photons has not been reported in any media.

In this paper, we demonstrate single-photon StFWM in a piece of optical fiber. The seeded photons are generated by SpFWM in the same fiber with a configuration of heralded single photon source (HSPS); hence they are true single photons (Fock states). The single-photon StFWM is confirmed by the time-resolved four-photon coincidence measurement and the variation of four-photon coincident counts under different delays between seeded photons and pump pulses. To show its potential for applications of photonic QIP, the performance of a quantum cloning machine based on this process is estimated according to the experiment results.

RESULTS

In the SpFWM and StFWM process, pairs of pump photons are annihilated, and pairs of correlated photons are generated, which are usually named as signal and idler photons, respectively. In the interaction picture, the simplified Hamiltonian for SpFWM and StFWM in an isotropic medium can be expressed as

$$\hat{H}_{\text{int}} \approx \hbar k \hat{a}_s^{\dagger} \hat{a}_i^{\dagger} + \text{hc} \tag{1}$$

where $\hbar$ is the reduced Planck constant. k is a nonlinear gain parameter, proportional to the nonlinear parameter $\chi^{(3)}$, pump power, and also includes the effect of the phase matching condition. $\hat{a}_s^{\dagger}$ ($\hat{a}_i^{\dagger}$) is the creation operator of signal (idler) photons, and hc is the hermitian conjugate.

In the SpFWM process, correlated photon pairs are generated with a vacuum state as the initial state, i.e.,

$$|\Psi_1\rangle = \exp\left(\frac{\hat{H}_{\text{int}}}{i\hbar}t\right)|00\rangle = |00\rangle + g|11\rangle \tag{2}$$

where $|mn\rangle$ is a photonic quantum state with m photons in the signal mode and n photons in the idler mode. $g = -ikt$, where t is the interaction time. Higher order terms have been neglected for $g \ll 1$. On the basis of this process, various complex photonic quantum states have been realized by coherent manipulation and superposition of the generated correlated state.[21−29]

In the StFWM process, the initial states of the signal or idler modes are no longer vacuum states. In this paper, we focus on the StFWM process with single photons in one mode as the initial state. Assuming that there are single photons in the signal mode as the seeded photons, the input state is $|10\rangle$. After the FWM process, the output state can be expressed as

$$|\Psi_2\rangle = \exp\left(\frac{\hat{H}_{\text{int}}}{i\hbar}t\right)|10\rangle = |10\rangle + \sqrt{2}g|21\rangle \tag{3}$$

Comparing with the output state of the SpFWM process shown in eq 2, there is an increase in the probability of generating photon pairs by a factor of 2 due to the seeded photons. The generated signal photons are in the same mode with the seeded signal photons, and the idler photons are also correlated with the two signal photons.

Experiment. The experiment is designed to demonstrate single-photon StFWM. True single photons are generated by an HSPS based on the SpFWM process in a piece of dispersion-shifted fiber (DSF). Then the heralded single photons are reflected back to the DSF as seeded photons with the pulsed pump light. By adjusting the time delay between the seeded photons and pump pulses (seed−pump delay) to make them overlap with each other, single-photon StFWM would occur and new pairs of photons would be generated. By statistically analyzing the cumulative time stamps of the four photons (the heralding photons, the heralded photons (used as the seeded photons), and the two photons generated by the StFWM process), time-resolved four-photon coincidence measurement can be realized. Here the DSF is used as the nonlinear medium since its nonlinear interaction length can be very long due to the waveguide nature and the low loss property. On the other hand, its zero dispersion wavelength is near 1.5 μm, which is preferred to realize SpFWM/StFWM at the telecom band. A degenerate pumping scheme is used so FWM Bragg scattering would not occur. According to eq 3, comparing with the SpFWM process (in the same nonlinear medium and under the same pump level), in the StFWM process, the photon pair generation rate would increase by a factor of 2 due to the single-photon stimulation. This property could be verified in two ways according to the results of the four-photon coincidence measurement. First, the coincidence to accidental-coincidence ratios are different in the cases with/without StFWM. Second, it can also be verified by the variation of four-photon coincident counts under different seed−pump delays.

The experiment setup is shown in Figure1. The pump source is realized by a mode-locked fiber laser, which has a repetition rate of 40 MHz, and three unbalanced Mach−Zenhder interferometers (MZIs) made by 50:50 optical beam splitters (50:50BS). The three unbalanced MZIs have different time delays between their arms, which are about 12.5, 6.2, and 3.1 ns, respectively. They are cascaded to multiplex the light pulses, leading to a repetition rate of 320 MHz, aimed at high photon-pair generation rates. A 100 GHz dense wavelength division multiplexer (DWDM, F_{p1}) is used as an optical filter to select the pump light with the center wavelength (1552.52 nm) and narrow its line width (0.3 nm). After being amplified by an erbium-doped fiber amplifier, an optical filter (F_{p2}) with a high extinction ratio (>120 dB) made by cascaded DWDM devices is used to suppress noise photons at the signal and idler wavelengths. The pump pulses are injected into a piece of DSF through an optical circulator to generate correlated photon pairs via the SpFWM process. The DSF, with a length of 280 m, is cooled to 2 K and placed in a Gifford−Mcmahon cryocooler shared by superconducting nanowire single-photon detectors (SNSPDs). Such a low operation temperature aims to suppress noise photons generated by the spontaneous Raman scattering in the fiber.[13] The filters for signal photons (F_s, central wavelength: 1549.32 nm) and for idler photons (F_{i1},

DOI: 10.1021/acsphotonics.6b01020
ACS Photonics 2017, 4, 746−753

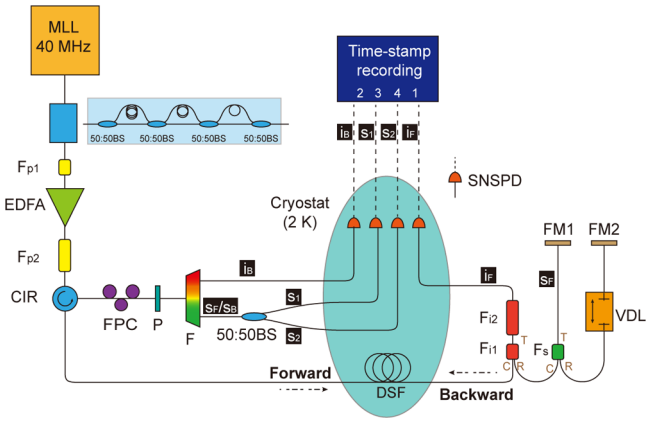

Figure 1. Experiment setup. MLL: mode-locked pulsed laser; 50:50BS: 50%:50% optical beam splitter; F_{p1}, F_{p2}, F_{i1}, F_{i2}, F_s, F: filters realized by (cascaded) 3-port 100 GHz DWDMs; CIR: optical circulator; FPC: fiber polarization controller; FM: Faraday mirror; VDL: variable optical delay line; P: polarizer; SNSPD: superconducting nanowire single-photon detector. C (T, R): common (transmission, reflection) port of DWMD devices.

central wavelength 1555.75 nm) are used to separate the signal photons, idler photons, and the residual pump. These filters are realized by cascaded 3-port DWDM devices. The idler photons are detected using a SNSPD (SNSPD1) after a DWDM-based filter (F_{i2}) with a high extinction ratio. The signal photons and the residual pump pulses are reflected back to the DSF by two Faraday mirrors (FM1, FM2), respectively, which also guarantees that they are in the same polarization state when propagating backward in the DSF.[40] Through a variable optical delay line (VDL), the delay between reflected signal photons and pump pulses (seed−pump delay) can be adjusted. The forward SpFWM process is used as an HSPS in which the signal photons are heralded by the idler photons. The coincidence to accidental-coincidence ratio is 58.2 ± 0.4, with a conditional second-order correlation $g^2(0) = 0.061 \pm 0.0007$.

The reflected signal photons, being seeded photons, would stimulate the FWM process backward pumped by the reflected pumps when they are temporally overlapped. The seeded photons and the signal and idler photons generated in the backward FWM process are separated by a filter module. Before the filter module, a polarizer and a fiber polarization controller are used to block the noise photons, with the polarization perpendicular to the pump light, which is mainly due to the spontaneous Raman scattering in the fiber pigtails of the optical devices outside the cryostat. A 50:50 beam splitter (BS) is used to probabilistically split the seeded and the stimulated signal photons and direct them to two SNSPDs. The SNSPD detection efficiency is about 30% for each channel in the experiment. The loss of the DSF is about 3 dB (the loss increases in the cryostat). The insertion losses of filters F and F_{i2} are about ∼2 dB, while the losses of F_s and F_{i1} are fairly small (0.2−0.3 dB). After being detected by SNSPDs, their channel numbers and arrival time stamps are recorded using a four-channel time-correlated single-photon-counting module. The data are postprocessed using a personal computer to fulfill the time-resolved four-photon coincidence measurement.

Time-Resolved Four-Photon Coincidence Measurement. The idler photons in the forward SpFWM process, the

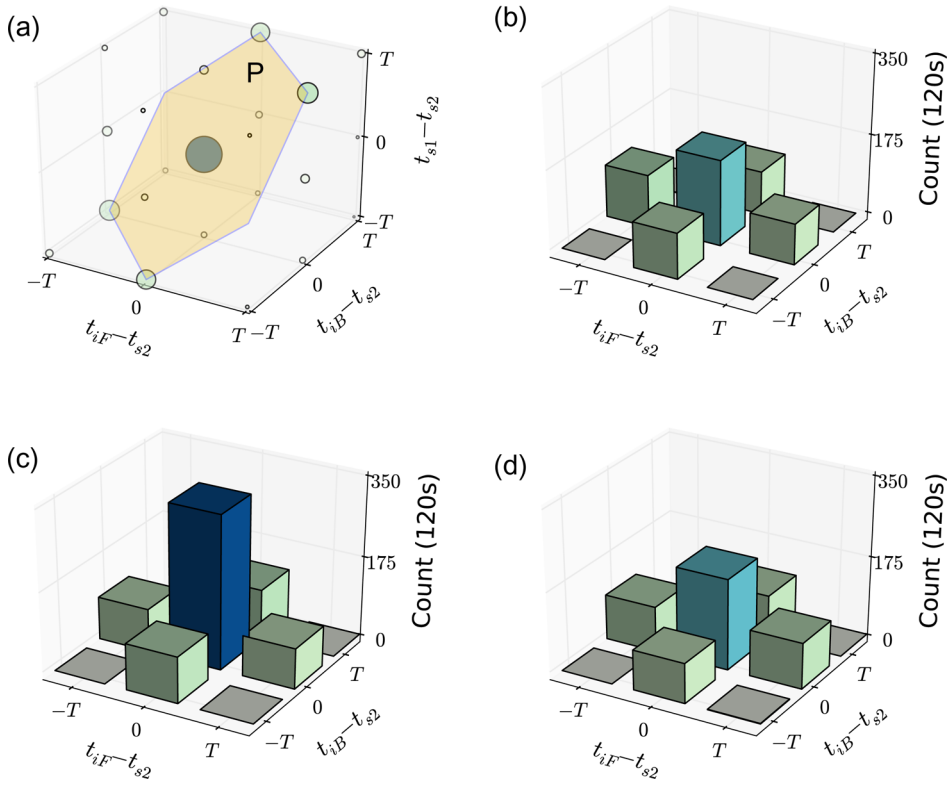

Figure 2. Results of time-resolved four-photon coincidence measurement. (a) Four-photon coincidence related to the delays of the recorded single-photon events (t_i: time stamps of single-photon events in the $i \in \{i_F, i_B, s_1, s_2\}$ channel, as shown in Figure 1). Only at some specific bins are there obvious four-photon coincident counts. (b−d) Four-photon coincidence distribution in the plane $t_{s1} = t_{iF} + t_{iB} - t_{s2}$ in (a). (b−d) Results of different seed−pump delays τ. (b) $\tau = -18.98$ ps; (c) $\tau = 0.62$ ps; (d) $\tau = 21.62$ ps. T is the repetition period of the pump.

DOI: 10.1021/acsphotonics.6b01020
ACS Photonics 2017, 4, 746−753

idler photons in the backward FWM process, and the two signal photons are labeled as i_F, i_B, s_1, s_2, respectively. The time stamps are denoted as t_{iF}, t_{iB}, t_{s1}, and t_{s2}, respectively. The photon counting rates in the four channels are 2.8, 0.5, 0.5, and 0.8 MHz, respectively. Since four photons are involved, three time delays, $t_{iF} - t_{s2}$, $t_{iB} - t_{s2}$, and $t_{s1} - t_{s2}$, are used as temporal variables for the four-photon coincidences. By statistically analyzing the cumulatively recorded time stamps of photons in the four channels in 120 s, we can calculate the four-photon coincident counts with different delays ($t_{iF} - t_{s2}$, $t_{iB} - t_{s2}$, and $t_{s1} - t_{s2}$). In the experiment, the time-stamps are recorded with a resolution of 1 ps, while the timing jitters of the SNSPDs are about 70 ps. For simplifying the calculation of the coincident counts, the time bin width is set to 2.56 ns, which is much larger than the timing jitters of SNSPD, but smaller than the period of pump pulses (T = 3.2 ns). Because of the low-noise photon level due to 2.2 K fiber-cooling and the low dark counting rates of SNSPDs (about 100 Hz), such a bin width would not deteriorate the noise properties in the coincidence measurement.[26] The results of the time-resolved four-photon coincidence measurement are shown in Figure 2. Figure 2a is a typical result of the four-photon coincidence distribution related to the three time delays among photons in the four channels. The bubble size is proportional to the four-photon coincident counts. It is obvious that the four-photon coincident counts are much larger than zero only at some specific bins. These bins satisfy the relation

$$(t_{iF} - t_{s2}) + (t_{iB} - t_{s1}) \equiv (t_{iF} - t_{s1}) + (t_{iB} - t_{s2}) = 0, \quad t_x = nT,\ x \in \{i_F, i_B, s_1, s_2\},\ n \in \mathbb{Z} \tag{4}$$

where T is the repetition period of the pump pulses. Equation 4 indicates that the four-photon coincidence is mainly due to two pairs of correlated photons generated by SpFWM or StFWM. The contributions of the noise photons and dark counts of the SNSPDs are quite small and can be neglected. Hence, we focus only on the coincident counts in these specific time bins satisfying eq 4, which is a scalar equation of a plane, as shown in Figure 2a.

In Figure 2b,c,d, we plot the distributions of four-photon coincidence in these time bins with different seed−pump delays τ, τ = −18.98 ps, τ = 0.62 ps, and τ = 21.62 ps, respectively. In the following, we denote the positon of time bins as (x, y), where $x = t_{iF} - t_{s2}$ and $y = t_{iB} - t_{s2}$.The central bars (0, 0) are defined as the four-photon true coincident counts (fpTCC), since they result from four photons generated by the same pump pulses, i.e., a pair in the forward process and another pair in the backward process, which would increase due to the single-photon stimulation in the backward FWM process when the seeded photons are overlapped with the pump pulses. In these figures, counts in the time bins ($\pm T$, 0), (0, $\pm T$) are also much larger than zero. The average count in these bins is defined as the four-photon accidental coincident count (fpACC), since these counts result from two pairs of photons generated by two adjacent pump pulses: one pair of photons generated in the forward SpFWM process driven by one pump pulse, another pair of photons generated in the backward FWM process by the other pump pulse. Because the seeded photons and the new generated photon pairs are not overlapped temporally in these cases, there would be no StFWM in the backward process for fpACC. The ratio of fpTCC and fpACC is defined by

$$R = \frac{1}{2}\frac{\text{fpTCC}}{\text{fpACC}} \tag{5}$$

where the factor $\frac{1}{2}$ is due to the probabilistic properties when the two signal photons are split at the 50:50 BS.

In Figure 2b and d, the time delays are larger than the coherence time of the seeded photons and the pump pulses, which are approximately t_c = 10 ps for both, determined by the bandwidths of corresponding optical filters (∼0.3 nm). Hence, in the backward FWM process, the seeded photons and pump pulses are not overlapped in these cases and there would not be single-photon StFWM (and also the increase of generation rate of photon pairs). According to the experiment data, the ratios are $R = 0.94 \pm 0.16$ for τ = −18.98 ps and $R = 1.04 \pm 0.18$ for τ = 21.62 ps, agreeing well with the theoretical value $R_{SpFWM} = 1$ for the case in which there is no single-photon StFWM in the backward process (shown in the Methods).

The condition is different for Figure 2c, in which the seed−pump delay is τ = 0.62 ps. In this case the reflected seeded photons and pump pulses are overlapped temporally, and an increase of the probability of generating photon pairs in the backward FWM process could be expected, due to the single-photon StFWM. Theoretical analysis (shown in the Methods section) shows that the fpTCC to fpACC ratio should be R_{StFWM} = 2 if perfect single-photon StFWM occurs in the backward process. The measured value is $R = 1.71 \pm 0.27$ according to the experimental results in Figure 2c, confirming the existence of the single-photon StFWM process. The deviation between the experimental results and the theoretical values may be due to the imperfect match of temporal and polarization modes between the seeded photons and the pump pulses due to temporal dispersion and birefringence of fibers.

Coincidence Measurement under Different Seed−Pump Delays. As mentioned earlier, by the variation of fpTCC at different seed−pump delay τ, the single-photon StFWM can be verified. In the experiment, except for the fpTCCs, we also measured the two-idler-photon coincidence ($i_F \wedge i_B$) under different seed−pump delays τ. In principle, both $i_F \wedge i_B$ and fpTCC would increase when seeded photons and pump pulses are overlapped, due to the single-photon StFWM. The results are shown in Figure 3. The coincident counts are measured in 120 s. The results of $i_F \wedge i_B$ are shown in Figure 3a. The $i_F \wedge i_B$ counts increase with $|\tau| \to 0$, indicating the existence of the single-photon StFWM. However, the increase factor is only 1.13 ± 0.003 according to the curve-fitting results, which is far lower than the photon pair generation rate increasing factor (2) due to single-photon StFWM. In our analysis, the increasing factors of $i_F \wedge i_B$ due to the StFWM are mainly limited by the transmission loss of the seeded photons. If the seeded photons are lost before injecting into the DSF, there would not be single-photon stimulation in the backward FWM process. The increase factor of $i_F \wedge i_B$ can be estimated as (see Methods for details)

$$R_{i_F \wedge i_B} = 1 + 10^{-L/10} \tag{6}$$

where L (dB) is the loss seeded photons pass, including the loss of DSF (3 dB), F_{i1} + F_s (0.5 dB), and FM1 (0.3 dB). Because of the double pass through DSF and F_{i1}/F_s, the total loss of seeded photons is L = 7.3 dB. Hence, the estimated two-idler-photon coincident count increase factor should be 1.18. The reasons that the measured value is less than the estimated value

DOI: 10.1021/acsphotonics.6b01020
ACS Photonics 2017, 4, 746−753

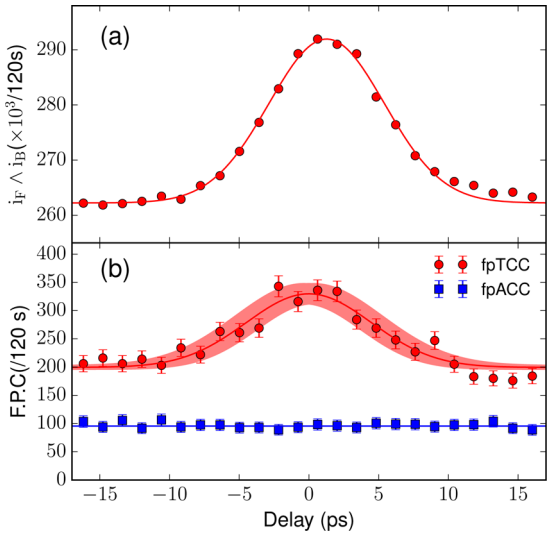

Figure 3. Coincidence variance under different seed−pump delays. (a) Two-idler-photon coincidence ($i_F \wedge i_B$); (b) four-photon coincident counts (fpTCC, red) and four-photon accidental coincident counts (fpACC, blue).

are similar to the discussion on the time-resolved four-photon coincidence measurement results.

Comparing with the $i_F \wedge i_B$ coincidence, the four-photon coincidence is more robust to the loss of the seeded photons, because of the postselection detection (only keeping the successfully heralded photons in the HSPS). The results are shown in Figure 3b, in which the red circles and blue squares denote the fpTCCs and fpACCs, respectively. The red line is the fitting curve of fpTCCs, and the blue horizontal line is the fitting line of the fpACCs. The red shadow around the fitted curve shows the uncertainties of the curve-fitting results. It can be seen that when the seed−pump delay τ approaches zero, the fpTCC increases obviously. The obvious increase of the fpTCC occurs only when the time delay τ is in a range of about 10.6 ps, which agrees well with the coherence time of the seeded photons and the pump pulses. As a comparison, the fpACCs are independent of the seed−pump time delay with small fluctuations only due to measurement uncertainties, indicating that the pump power is stable in the measurement.

According to the experimental results and the fitted curve shown in Figure 3b, the increasing factor of fpTCC due to the single-photon StFWM is

$$R' = \frac{C_{\tau=0}}{C_{\tau \gg t_c}} = 1.65 \pm 0.06 \tag{7}$$

where $C_{\tau=0}$ is the fpTCC at $\tau = 0$ and $C_{\tau \gg t_c}$ is the fpTCC when τ is much larger than the coherence time of seeded photons and pump pulses t_c. This increase verifies the single-photon StFWM in the backward FWM process. It can be seen that the increasing factor R' agrees well with the fpTCC to fpACC ratio R. Actually, R and R' are equivalent, because $C_{\tau \gg t_c}$ result from two pairs of photons by SpFWM in the forward and backward direction, similar to the fpACC. It should be noted that the fpTCC to fpACC ratio R is calculated only based on the results of the four-photon coincidence measurement when τ is close to zero. Hence the experiment could be simplified if only the fpTCC to fpACC ratio R is used to varify the single-photon StFWM, in which the seeded photons and pump light could be reflected together and the VDL is not required.

Estimation of the Performance of Universal Quantum Cloning Based on Single-Photon StFWM Process. One important application of the single-photon StFWM process is the universal quantum cloning. Although perfect cloning of an arbitrary quantum state is prohibited by quantum mechanics (the no-cloning theorem[41]), it has been proven that imperfect cloning of an arbitrary quantum state is possible. In the process of quantum cloning, fidelity is an important *figure of merit*, which is defined as $F = \langle \psi_{in} | \rho^{out} | \psi_{in} \rangle$, where $|\psi_{in}\rangle$ is the state to be cloned and ρ^{out} is the reduced density matrix of the output states. For a universal quantum cloning machine (UQCM), the fidelities are independent of the input state. If the fidelities of all ouput states are equal to each other, the process is called a symmetrical QCM. It has been proven[42] that in a symmetrical UQCM for two-state quantum systems, the upper bound of fidelity for cloning one qubit to produce two qubits ($1 \rightarrow 2$) is $\mathcal{F}_{1\rightarrow 2} = \frac{5}{6}$. If a UQCM can obtain the related theoretical bound, it is called an optimal UQCM. It has been proposed that the optimal UQCM can be realize by single-photon stimulated emission. The $1 \rightarrow 2$ UQCM based on single-photon stimulated parametric downconversion in second nonlinear crystals has been demonstrated in ref 36, which clones a qubit in the degree of freedom of polarization, with a fidelity of 81 ± 1%.

However, the lack of the observation of single-photon-stimulated FWM results in the lack of the demonstration of optimal UQCM on a third-order nonlinear platform, including nonlinear optical fibers and integrated waveguides.

In this paper, we demonstrate the single-photon StFWM. It can be realized in third-order nonlinear waveguides at the telecom band, such as optical fibers and silicon waveguides. It has great potential to realize UQCM at the telecom band. Here we provide an estimation of the upper limit of the fidelity if the single-photon StFWM process in the fibers of our experimental setup is used to realize a $1 \rightarrow 2$ UQCM (cloning time-bin qubit, for example). Acording to ref 36, the fidelity can be estimated by the value of R',

$$F = \frac{2R' + 1}{2R' + 2} = 81.1 \pm 0.4\% \tag{8}$$

which is very close to the theoretical upper bound of the fidelity of symmetrical $1 \rightarrow 2$ UQCM, 83.3%. It can be seen that the single-photon StFWM process has great potential for quantum information processing based on quantum cloning, especially the applications at the telecom band.

DISCUSSION

As a summary, in this paper we have demonstrated the true-single-photon StFWM process in a piece of DSF, which is placed in a 2 K cryostat to suppress the Raman noise effectively. The true single photons are generated by an HSPS based on the SpFWM process in the same fiber. We characterize the StFWM process by the time-resolved four-photon coincidence measurement. The StFWM process is demonstrated by the fpTCC to fpACC ratio $R = 1.71 \pm 0.27 > 1$ when the seeded photons and pump pulses are overlapped. The StFWM process is also characterized by the variation of four-photon coincident counts under different seed−pump delays. There is an increase by a factor of $1.65 \pm 0.06 > 1$ in the fpTCC when the seeded photons are overlapped with the pump pulses, which also

DOI: 10.1021/acsphotonics.6b01020
ACS Photonics 2017, 4, 746−753

confirms the existence of StFWM. This is the first demonstration of the true-single-photon StFWM process, and the process can be applied in QIP, extending the set of capable tasks based on an FWM process. As a typical example, the upper limit of the fidelity of a $1 \rightarrow 2$ UQCM based on the single-photon StFWM in our experiment is estimated to be $81.1 \pm 0.4\%$, close to the theoritical upper bound.

METHODS

Analysis of the fpTCC to fpACC Ratio. Timing relations of photons for different four-photon coincident counts are shown in Figure 4. As shown in Figure 4a, the fpTCC results

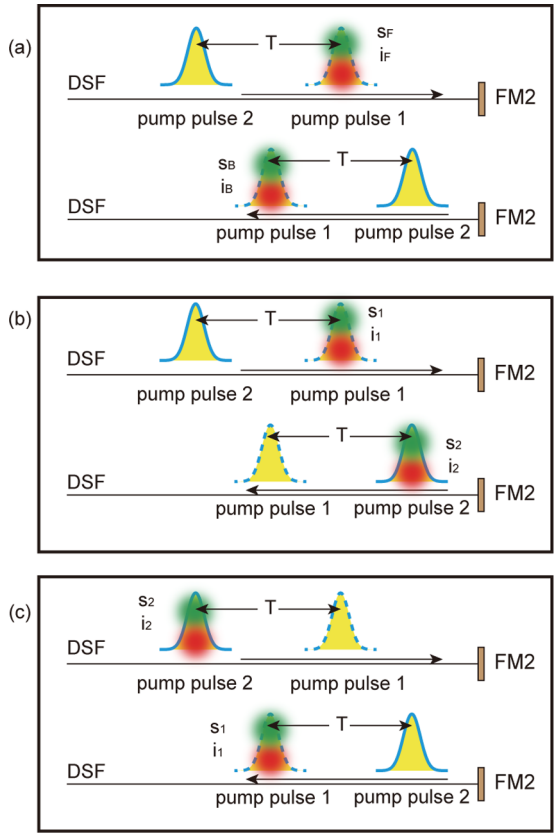

Figure 4. Timing relation of photons for different four-photon coincident counts. (a) Cases related to fpTCC. (b) One of the two cases related to fpACC, forward s_1 and i_1 and backward s_2 and i_2. (c) One of the two cases related to fpACC, backward s_1 and i_1 and forward s_2 and i_2.

from two photon pairs generated by a single pump pulse, one pair by the SpFWM process in the forward direction and the other pair by SpFWM or StFWM in the backward direction depending on the time delay between the seeded photons and the pump pulses. Assuming that r_1 is the photon pair generation rate in the forward direction and r_2 is that in the backward process, when the seed−pump delay is much larger than their coherence time, both the forward and the backward processes are SpFWM processes. The fpTCC rate will be

$$r_{\mathrm{fpTCC}} = \frac{1}{2}\eta r_1 r_2 \tag{9}$$

The factor $\frac{1}{2}$ comes from the fact that there is half the probability that the two signal photons will go to the same output port of the 50:50 BS and no four-photon coincidence count can be expected in this case. η is a coefficient related to the system collection efficiency, including the channel loss and detecting efficiencies of the SNSPDs. fpACCs are due to two pairs of photons generated by two adjacent pump pulses, one in the forward direction by one pump pulse and another in the backward direction by the other pump pulse. In the following, the two adjacent pump pulses are denoted as pulse 1 and pulse 2, and pulse 1 is in advance of pulse 2. The signal and idler photons generated by the pump pulse 1(2) are indexed by $s_1(s_2)$ and $i_1(i_2)$, respectively. The two pairs of photons are generated in the forward and backward direction in the DSF, and there are two cases as shown in Figure 4b,c. In one case (Figure 4b), s_1 and i_1 are generated in the forward direction and s_2 and i_2 are generated in the backward direction, denoted as forward s_1 and i_1 and backward s_2 and i_2. The other case (Figure 4c) is just the contrary and denoted as backward s_1 and i_1 and forward s_2 and i_2. The channels through which photons will go out and related probabilities are shown in Table 1. The cases in which four photons are detected in four different channels would result in fpACCs at specific time bins in Figure 2, which are indicated by (x, y), $x, y \in \{0, \pm T\}$ with $t_{i_F} - t_{s_2} = x$ and $t_{i_B} - t_{s_2} = y$.

The four terms of fpACC in Table 1 are related to the four accidental coincident count bars in Figure 2b,c,d. Hence, according to Table 1, for every fpACC bar, the fpACC rate is

$$r_{\mathrm{fpACC}} = \eta r_1 r_2 / 4 \tag{10}$$

According to the definition (eq 5), for the case when only the SpFWM process occurs in the backward direction, the theoretical prediction of R would be

$$R_{\mathrm{SpFWM}} = \frac{1}{2}\frac{r_{\mathrm{fpTCC}}}{r_{\mathrm{fpACC}}} \equiv 1 \tag{11}$$

On the other hand, if the seeded photons and the pump pulses are overlapped temporally, the StFWM process would occur in the backward direction; hence, the generation rate of photon pairs in the backward direction would increase by a factor of 2, i.e., $r_2 \rightarrow r_2^* = 2r_2$, according to eq 3, while the

Table 1. Probabilities of All Possible Outputs of the Four Photons and Their Corresponding Bins of Accidental Coincident Counts

	forward s_1 and i_1, backward s_2 and i_2				backward s_1 and i_1, forward s_2 and i_2			
i_1	1	1	1	1	2	2	2	2
s_1	3	3	4	4	3	3	4	4
i_2	2	2	2	2	1	1	1	1
s_2	4	3	3	4	4	3	3	4
prob	1/4	1/4	1/4	1/4	1/4	1/4	1/4	1/4
bin	$(-T, 0)$	no ACC	$(0, T)$	no ACC	$(0, -T)$	no ACC	$(T, 0)$	no ACC

DOI: 10.1021/acsphotonics.6b01020
ACS Photonics 2017, 4, 746−753

fpACC rates remain unchanged. Hence, the theoretical prediction of R, when the StFWM process occurs in the backward direction, would be

$$R_{\mathrm{StFWM}} = \frac{1}{2}\frac{\eta r_1 r_2^{*}/2}{\eta r_1 r_2/4} \equiv 2 \tag{12}$$

Relation between Two-Idler-Photon Coincidence Increasing Factor and the Loss of Seeded Photons. The two-idler-photon coincidence measurement records the events in which the two idler photons i_F and i_B are detected simultaneously. It can be expected that the two-idler-photon coincidence would increase when the seed−pump delay τ is close to zero, due to the single-photon StFWM. However, the increase factor is impacted by the loss of the seeded photons. If the loss of the seeded photons is L (dB), under the condition that the i_F photons are detected, the probability that there are seeded photons is $P(\mathrm{seed}|i_F) = 10^{-L/10}$. If the seed−pump delay is larger than the coherence time of pump pulses or the seeded photons are lost before being injected into the DSF, only the SpFWM could occur in the backward FWM process. The generation rate of photon pairs is indicated by G (the unit is $(\mathrm{pump\ pulse})^{-1}$). On the other hand, if the seed−pump delay τ is close to zero, the single-photon StFWM would occur when seeded photons are inject into the fiber. The generation rate of photon pairs is $2G$ ($(\mathrm{pump\ pulse})^{-1}$) according to eq 3. Hence, when the seed−pump delay is zero, under the condition that i_F is detected, the average generation rate of photon pairs is $P(\mathrm{seed}|i_F)2G + (1 - P(\mathrm{seed}|i_F))G = (1 + P(\mathrm{seed}|i_F))G$. Therefore, the increasing factor of the two-idler-photon coincident counts due to the single-photon StFWM can be expressed as

$$R_{i_F \wedge i_B} = \frac{(1 + P(\mathrm{seed}|i_F))G}{G} \equiv 1 + 10^{-L/10} \tag{13}$$

AUTHOR INFORMATION

Corresponding Author

*E-mail: zwei@tsinghua.edu.cn.

ORCID

Wei Zhang: 0000-0002-6848-6807

Notes

The authors declare no competing financial interest.

ACKNOWLEDGMENTS

This work was supported by the 973 Programs of China under Contract Nos. 2013CB328700 and 2011CBA00303, the National Natural Science Foundation of China under Contract Nos. 61575102, 91121022, and 61621064, Tsinghua University Initiative Scientific Research Program under Contract No. 20131089382, and Strategic Priority Research Program (B) of the Chinese Academy of Sciences (XDB04020100).

REFERENCES

(1) Agrawal, G. P. *Nonlinear Fiber Optics*; Academic Press, 2007.

(2) Carman, R. L.; Chiao, R. Y.; Kelley, P. L. Observation of Degenerate Stimulated Four-Photon Interaction and Four-Wave Parametric Amplification. *Phys. Rev. Lett.* **1966**, *17*, 1281−1283.

(3) Tong, Z.; Lundström, C.; Andrekson, P.; McKinstrie, C.; Karlsson, M.; Blessing, D.; Tipsuwannakul, E.; Puttnam, B.; Toda, H.; Grüner-Nielsen, L. Towards ultrasensitive optical links enabled by low-noise phase-sensitive amplifiers. *Nat. Photonics* **2011**, *5*, 430−436.

(4) Yariv, A.; Pepper, D. M. Amplified reflection, phase conjugation, and oscillation in degenerate four-wave mixing. *Opt. Lett.* **1977**, *1*, 16−18.

(5) Fukuda, H.; Yamada, K.; Shoji, T.; Takahashi, M.; Tsuchizawa, T.; Watanabe, T.; Takahashi, J.-i.; Itabashi, S.-i. Four-wave mixing in silicon wire waveguides. *Opt. Express* **2005**, *13*, 4629−4637.

(6) Salem, R.; Foster, M. A.; Turner, A. C.; Geraghty, D. F.; Lipson, M.; Gaeta, A. L. Signal regeneration using low-power four-wave mixing on silicon chip. *Nat. Photonics* **2008**, *2*, 35−38.

(7) Gu, T.; Petrone, N.; McMillan, J. F.; van der Zande, A.; Yu, M.; Lo, G.-Q.; Kwong, D.-L.; Hone, J.; Wong, C. W. Regenerative oscillation and four-wave mixing in graphene optoelectronics. *Nat. Photonics* **2012**, *6*, 554−559.

(8) Sharping, J. E.; Fiorentino, M.; Kumar, P. Observation of twin-beam-type quantum correlation in optical fiber. *Opt. Lett.* **2001**, *26*, 367−369.

(9) Agarwal, G. Generation of pair coherent states and squeezing via the competition of four-wave mixing and amplified spontaneous emission. *Phys. Rev. Lett.* **1986**, *57*, 827.

(10) Boyer, V.; Marino, A. M.; Pooser, R. C.; Lett, P. D. Entangled images from four-wave mixing. *Science* **2008**, *321*, 544−547.

(11) Wang, L.; Hong, C.; Friberg, S. Generation of correlated photons via four-wave mixing in optical fibres. *J. Opt. B: Quantum Semiclassical Opt.* **2001**, *3*, 346.

(12) Fiorentino, M.; Voss, P. L.; Sharping, J. E.; Kumar, P. All-fiber photon-pair source for quantum communications. *IEEE Photonics Technol. Lett.* **2002**, *14*, 983−985.

(13) Takesue, H.; Inoue, K. 1.5-μm band quantum-correlated photon pair generation in dispersion-shifted fiber: suppression of noise photons by cooling fiber. *Opt. Express* **2005**, *13*, 7832−7839.

(14) Sharping, J. E.; Lee, K. F.; Foster, M. A.; Turner, A. C.; Schmidt, B. S.; Lipson, M.; Gaeta, A. L.; Kumar, P. Generation of correlated photons in nanoscale silicon waveguides. *Opt. Express* **2006**, *14*, 12388−12393.

(15) He, J.; Bell, B. A.; Casas-Bedoya, A.; Zhang, Y.; Clark, A. S.; Xiong, C.; Eggleton, B. J. Ultracompact quantum splitter of degenerate photon pairs. *Optica* **2015**, *2*, 779−782.

(16) Gentry, C. M.; et al. Quantum-correlated photon pairs generated in a commercial 45 nm complementary metal-oxide semiconductor microelectronic chip. *Optica* **2015**, *2*, 1065−1071.

(17) Harris, N. C.; Grassani, D.; Simbula, A.; Pant, M.; Galli, M.; Baehr-Jones, T.; Hochberg, M.; Englund, D.; Bajoni, D.; Galland, C. Integrated source of spectrally filtered correlated photons for large-scale quantum photonic systems. *Phys. Rev. X* **2014**, *4*, 041047.

(18) Kumar, R.; Ong, J. R.; Savanier, M.; Mookherjea, S. Controlling the spectrum of photons generated on a silicon nanophotonic chip. *Nat. Commun.* **2014**, *5*.548910.1038/ncomms6489

(19) Lu, X.; Rogers, S.; Gerrits, T.; Jiang, W. C.; Nam, S. W.; Lin, Q. Heralding single photons from a high-Q silicon microdisk. *Optica* **2016**, *3*, 1331−1338.

(20) Azzini, S.; Grassani, D.; Galli, M.; Gerace, D.; Patrini, M.; Liscidini, M.; Velha, P.; Bajoni, D. Stimulated and spontaneous four-wave mixing in silicon-on-insulator coupled photonic wire nano-cavities. *Appl. Phys. Lett.* **2013**, *103*, 031117.

(21) Li, X.; Voss, P. L.; Sharping, J. E.; Kumar, P. Optical-fiber source of polarization-entangled photons in the 1550 nm telecom band. *Phys. Rev. Lett.* **2005**, *94*, 053601.

(22) Fan, J.; Eisaman, M.; Migdall, A. Quantum state tomography of a fiber-based source of polarization-entangled photon pairs. *Opt. Express* **2007**, *15*, 18339−18344.

(23) Liao, K.; Yan, H.; He, J.; Du, S.; Zhang, Z.-M.; Zhu, S.-L. Subnatural-linewidth polarization-entangled photon pairs with controllable temporal length. *Phys. Rev. Lett.* **2014**, *112*, 243602.

(24) Xiong, C.; et al. Compact and reconfigurable silicon nitride time-bin entanglement circuit. *Optica* **2015**, *2*, 724−727.

(25) Takesue, H. Long-distance distribution of time-bin entanglement generated in a cooled fiber. *Opt. Express* **2006**, *14*, 3453−3460.

DOI: 10.1021/acsphotonics.6b01020
ACS Photonics 2017, 4, 746−753

(26) Dong, S.; Zhou, Q.; Zhang, W.; He, Y.; Zhang, W.; You, L.; Huang, Y.; Peng, J. Energy-time entanglement generation in optical fibers under CW pumping. *Opt. Express* **2014**, *22*, 359−368.
(27) Grassani, D.; Azzini, S.; Liscidini, M.; Galli, M.; Strain, M. J.; Sorel, M.; Sipe, J.; Bajoni, D. Micrometer-scale integrated silicon source of time-energy entangled photons. *Optica* **2015**, *2*, 88−94.
(28) Rogers, S.; Mulkey, D.; Lu, X.; Jiang, W. C.; Lin, Q. High Visibility Time-Energy Entangled Photons from a Silicon Nanophotonic Chip. *ACS Photonics* **2016**, *3*, 1754−1761.
(29) Suo, J.; Dong, S.; Zhang, W.; Huang, Y.; Peng, J. Generation of hyper-entanglement on polarization and energy-time based on a silicon micro-ring cavity. *Opt. Express* **2015**, *23*, 3985−3995.
(30) Garay-Palmett, K.; McGuinness, H.; Cohen, O.; Lundeen, J.; Rangel-Rojo, R.; U'ren, A.; Raymer, M.; McKinstrie, C.; Radic, S.; Walmsley, I. Photon pair-state preparation with tailored spectral properties by spontaneous four-wave mixing in photonic-crystal fiber. *Opt. Express* **2007**, *15*, 14870−14886.
(31) McKinstrie, C. J.; Harvey, J. D.; Radic, S.; Raymer, M. G. Translation of quantum states by four-wave mixing in fibers. *Opt. Express* **2005**, *13*, 9131−9142.
(32) McGuinness, H. J.; Raymer, M. G.; McKinstrie, C. J.; Radic, S. Quantum Frequency Translation of Single-Photon States in a Photonic Crystal Fiber. *Phys. Rev. Lett.* **2010**, *105*, 093604.
(33) Li, Q.; Davanço, M.; Srinivasan, K. Efficient and low-noise single-photon-level frequency conversion interfaces using silicon nanophotonics. *Nat. Photonics* **2016**, *10*, 406.
(34) De Martini, F.; Bužek, V.; Sciarrino, F.; Sias, C. Experimental realization of the quantum universal NOT gate. *Nature* **2002**, *419*, 815−818.
(35) Simon, C.; Weihs, G.; Zeilinger, A. Optimal quantum cloning via stimulated emission. *Phys. Rev. Lett.* **2000**, *84*, 2993.
(36) Lamas-Linares, A.; Simon, C.; Howell, J. C.; Bouwmeester, D. Experimental quantum cloning of single photons. *Science* **2002**, *296*, 712−714.
(37) De Martini, F. Amplification of Quantum Entanglement. *Phys. Rev. Lett.* **1998**, *81*, 2842−2845.
(38) Lamas-Linares, A.; Howell, J. C.; Bouwmeester, D. Stimulated emission of polarization-entangled photons. *Nature* **2001**, *412*, 887−890.
(39) Agarwal, A.; Dailey, J. M.; Toliver, P.; Peters, N. A. Entangled-pair transmission improvement using distributed phase-sensitive amplification. *Phys. Rev. X* **2014**, *4*, 041038.
(40) Kersey, A.; Marrone, M.; Davis, M. Polarisation-insensitive fibre optic Michelson interferometer. *Electron. Lett.* **1991**, *27*, 518−520.
(41) Wootters, W. K.; Zurek, W. H. A single quantum cannot be cloned. *Nature* **1982**, *299*, 802−803.
(42) Scarani, V.; Iblisdir, S.; Gisin, N.; Acín, A. Quantum cloning. *Rev. Mod. Phys.* **2005**, *77*, 1225−1256.

DOI: 10.1021/acsphotonics.6b01020
ACS Photonics 2017, 4, 746−753